Strangeness enhancements and the muon excess in extensive air showers

1. The fireball and "strangeball"models
2. Application to Pierre Auger data
3. Implications for LHC measurements

based on work by Manshanden, Garzelli and Sigl,
JCAP 02 (2023) 017 [arXiv:2208.04266]

DFG Deutsche Forschungsgemeinschaft

PROJEKTTRÄGER FÜR DAS
Bundesministerium für Bildung und Forschung

CLUSTER OF EXCELLENCE
QUANTUM UNIVERSE

UHH Universität Hamburg
DER FORSCHUNG | DER LEHRE | DER BILDUNG

Günter Sigl
II. Institut theoretische Physik, Universität Hamburg

Definition of Fireball Model

A high-multiplicity fireball is created by a nuclear fragment if their energy is larger than a fraction of the projectile energy, see Anchordoqui et al., PRD 95 (2017) 063005, JHEP 34 (2022) 19 [arXiv:2202.03095]

$$E_{\rm frag} > f_{\rm thres} E_{\rm proj} \,,$$

This occurs with a probability

$$p(E) = \begin{cases} 0 \,, & \text{if } E < E_{\rm min}, \\ \left[\dfrac{\log(E/E_{\rm min})}{\log(E_{\rm max}/E_{\rm min})} \right]^n , & \text{if } E_{\rm min} < E < E_{\rm max}, \\ 1 \,, & \text{if } E > E_{\rm max} \,, \end{cases}$$

which is related to the core-corona model (core=fireball), see e.g. Baur et al., PRD 107 (2023) 094013 [arXiv:1902.09265]

If $f_{\rm thresh} < 1$ a fireball will form, a plasma consisting of deconfined up and down quarks and gluons. At high baryochemical potential gluons fragment into strange quarks, enhancing strange secondaries and suppressing neutral pion production. This can be mimicked by swapping all pions and kaons while conserving energy, direction of momentum and charge.

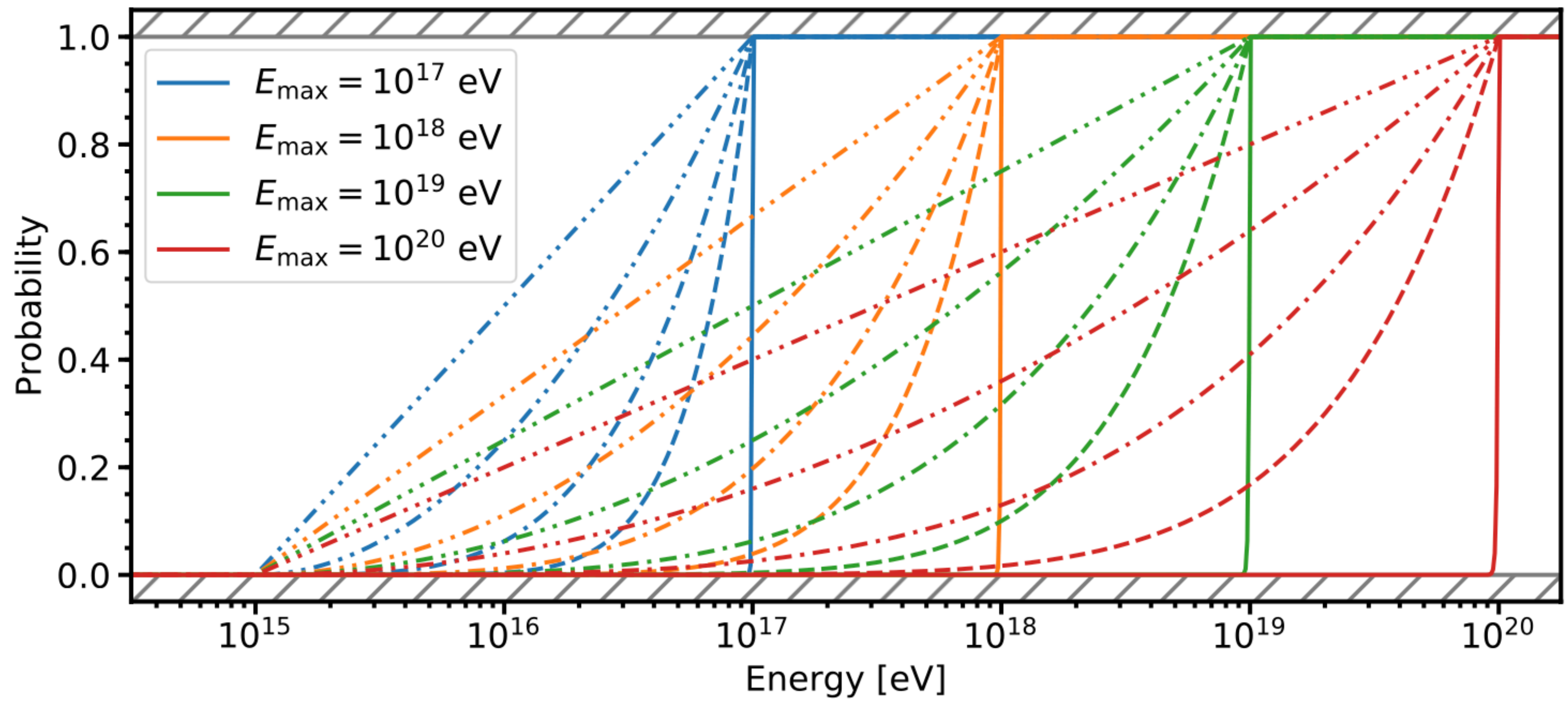

Figure 5.5: Various realizations of the parametrized (Eq. 5.3) probability of initiating a fireball as a function of the projectile energy. The minimum energy $E_{min} = 10^{15}$ eV is fixed whereas the maximum energy E_{max} is set to 10^{17} eV (blue), 10^{18} eV (orange), 10^{19} eV (green), and 10^{20} eV (red). The n-parameter is set to 1 (triple-dot dashed), 2 (double-dot dashed), 4 (dot dashed), 8 (dashed), and 1000 (solid). Manshanden, PhD thesis 2021

More detailed pion-kaon swapping criteria, based on secondary particle energy range, pseudorapidity and nucleus baryon number have been entertained in Anchordoqui et al., JHEP 34 (2022) 19 [arXiv:2202.03095]

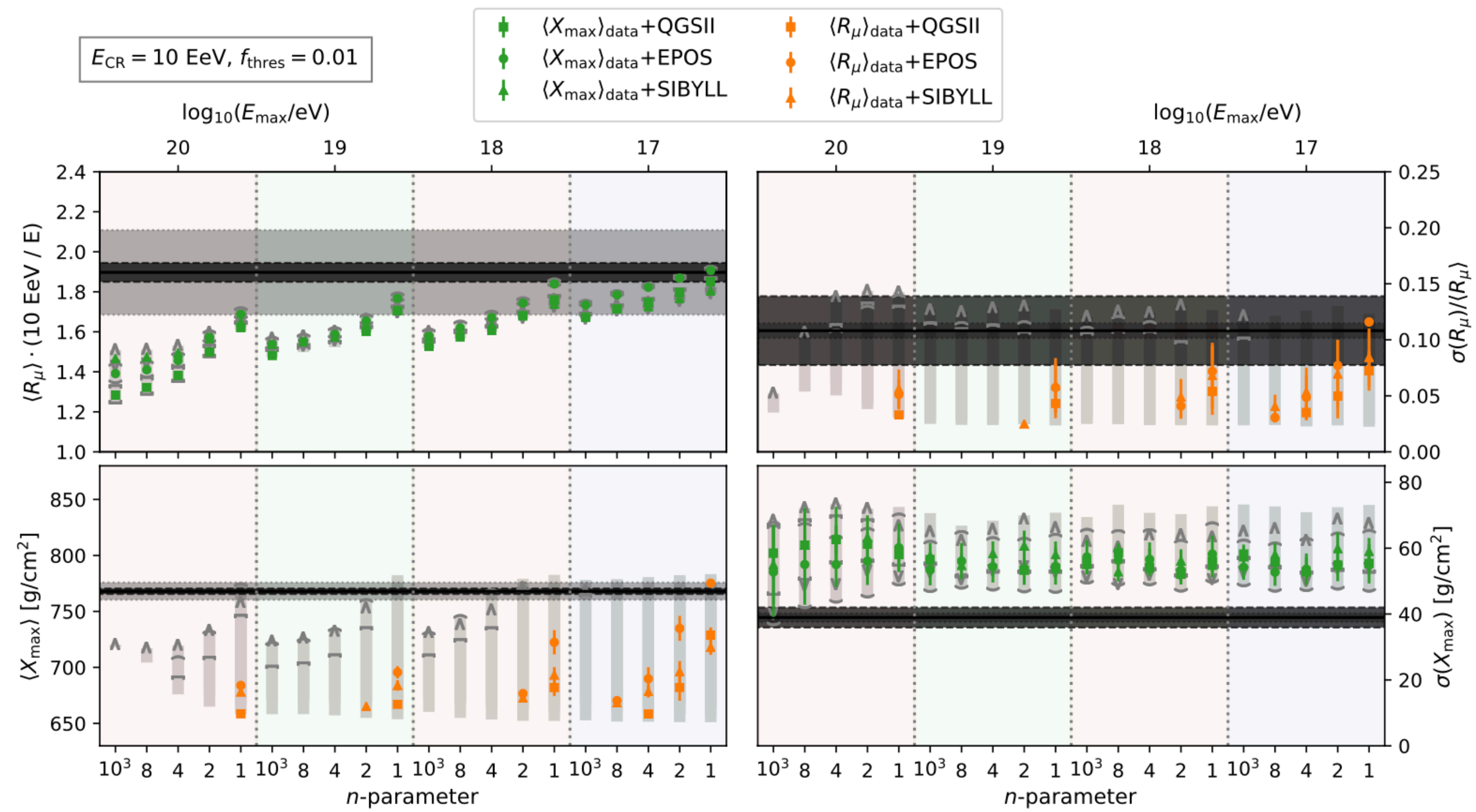

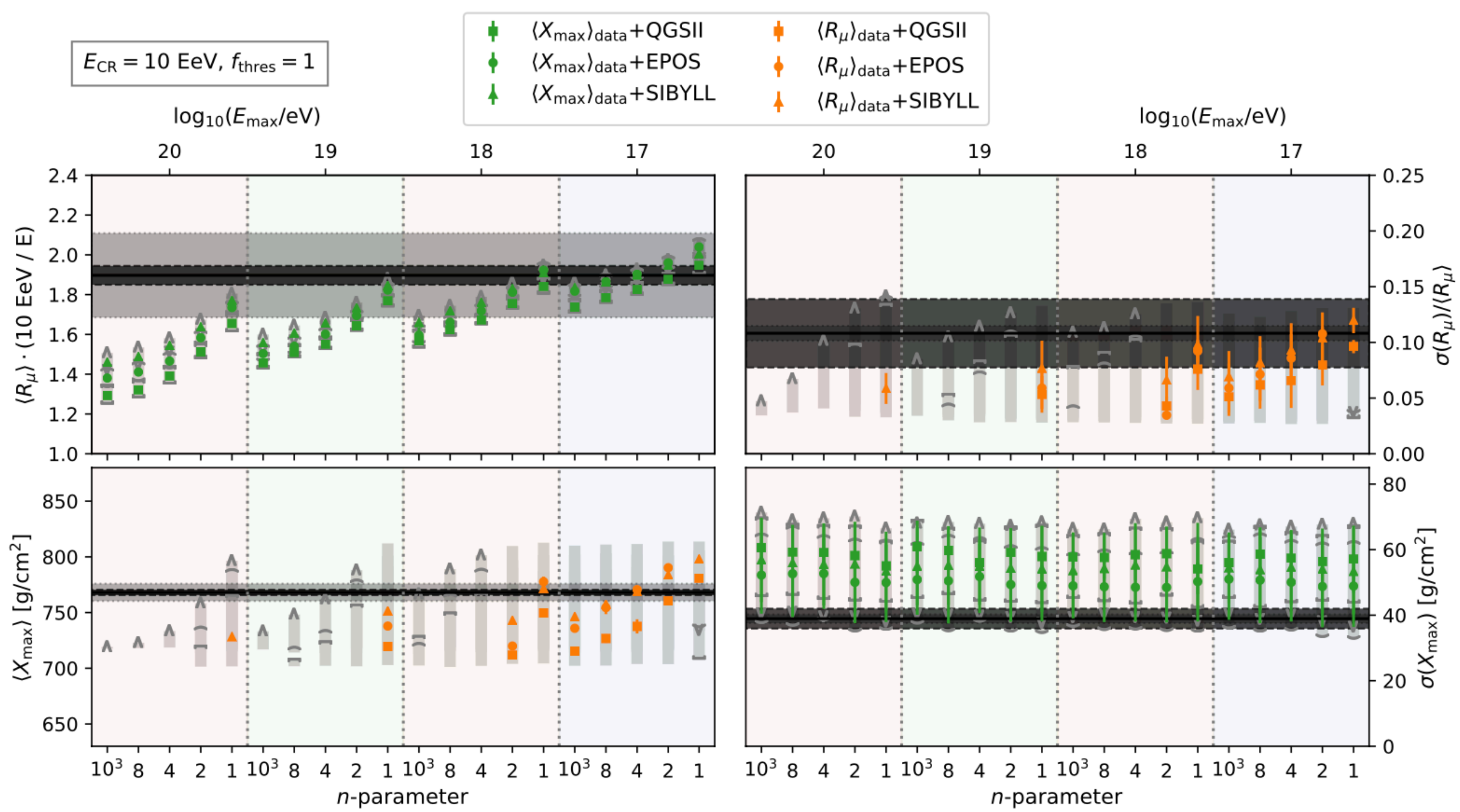

Main point:

models with $f_{\mathrm{thresh}} < 1$ don't fit the air shower data due to tension between $X_{\max}$ and its fluctuations

Definition of Strangeball Model

In the strangeball model no plasma forms, $f_{\rm thres} = 1$. The effective average fraction $r_{\rm eff} = E_{\rm had}/E_{\rm proj}$ of projectile energy $E_{\rm proj}$ going into the hadronic channel can be written as (Manshanden, Garzelli and Sigl, JCAP 02 (2023) 017 [arXiv:2208.04266])

$$r_{\rm eff}(E) \equiv [1 - p(E)]r_{\rm SM} + p(E)r_{\rm sb}\,,$$

with $r_{\rm SM}$ and $r_{\rm sb}$ the respective fractions for Standard Model interactions and strange balls, respectively. With this one can estimate the muon number in a proton induced air shower of primary energy E_0 as

$$N_\mu \simeq \left(\frac{E_0}{E_c}\right)\left(\frac{r_{\rm sb}}{r_{\rm SM}}\right)^{p(E_0)/2} \exp\left[\int_0^{k_c} \log\{r_{\rm eff}(E)\}\, dk + \Delta_{\rm disc}\right]\,,$$

where $E(k)$ can be deduced iteratively from $E_{k+1} = E_k/n_{\rm mult}(E_k)$, with the multiplicity parametrised as

$$n_{\rm mult}(E) = n_{\rm scale}\left(\frac{E}{1\ {\rm GeV}}\right)^b\,.$$

Parameters for analytical muon number calculation

		r_{SM}	r_{sb}	n_{scale}	b	E_c [GeV]
CRMC	QGSJetII-04	0.781	0.937	5.69	0.193	—
	EPOS-LHC	0.788	0.930	7.70	0.166	—
	Sibyll-2.3c	0.803	0.921	6.74	0.173	—
Conex	QGSJetII-04	0.509	0.720	968	$8.68 \cdot 10^{-2}$	136
	EPOS-LHC	0.550	0.764	3820	$2.58 \cdot 10^{-3}$	154
	Sibyll-2.3d	0.565	0.736	3230	$3.92 \cdot 10^{-5}$	151

Table 2. Estimates of the parameters related to physical quantities for the evaluation of eq. (4.5), using both CRMC and Conex simulations and various hadronic interaction models.

The strangeball model has the additional parameters E_{min}, E_{max} and n.

In contrast to the core-corona model where both core and corona contribute to interactions with $p(E) \to \omega_{\mathrm{core}}$ and $1 - \omega_{\mathrm{core}}$, respectively, a strangeball occurs with probability $p(E)$.

Muon Number and Pierre Auger data

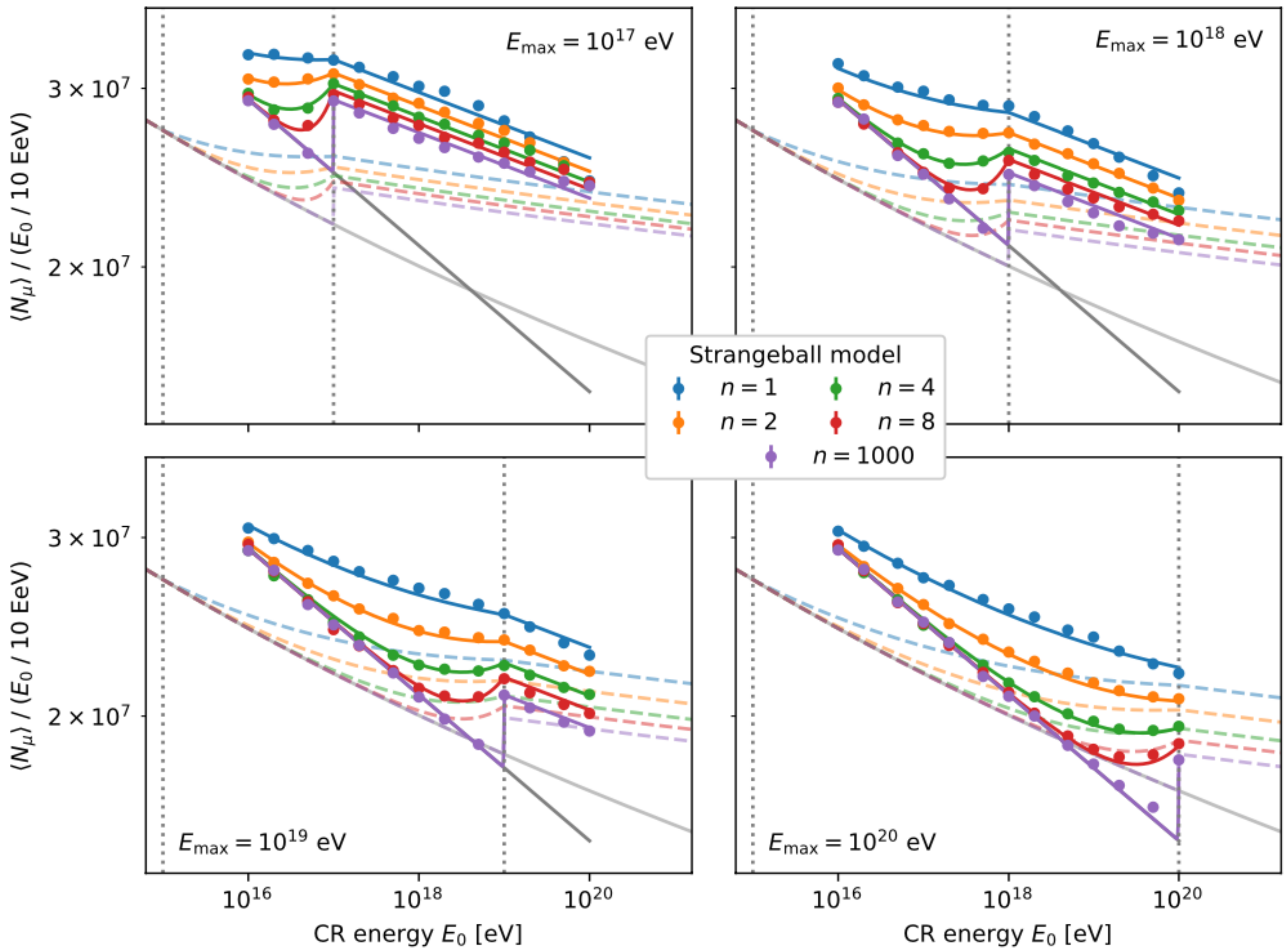

Figure 4. Energy dependence of the average muon number for various strangeball settings with EPOS-LHC as obtained with CONEX simulations (data points) fitted with eq. (4.5) (solid lines), and using CRMC-inferred parameters directly with eq. (4.5) (dashed lines). The gray lines correspond to the no strangeball case, and we fixed $E_{min} = 10^{15}$ eV.

data points = CONEX simulations

solid lines = fit to simulations

dashed lines = analytical estimates

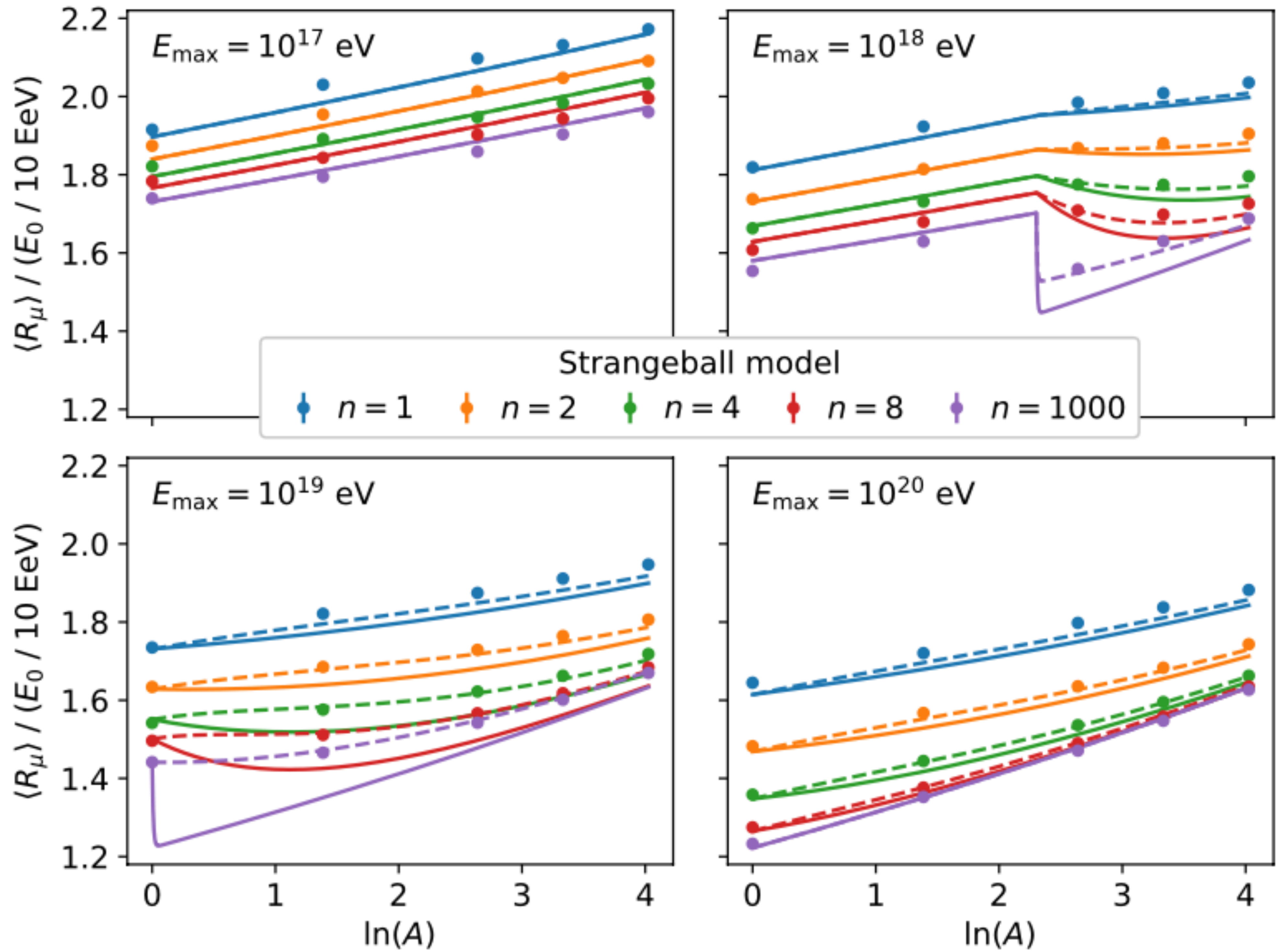

Figure 5. Mass dependence of the average muon number at $E_0 = 10\,\mathrm{EeV}$ for various strangeball settings obtained from EPOS-LHC CONEX simulations (data points) and compared with our analytic model (eq. (4.5) with CONEX parameters of table 2) by applying the superposition principle (eq. (4.9), solid lines) and when including our correction factor (with eq. (4.10), dashed lines).

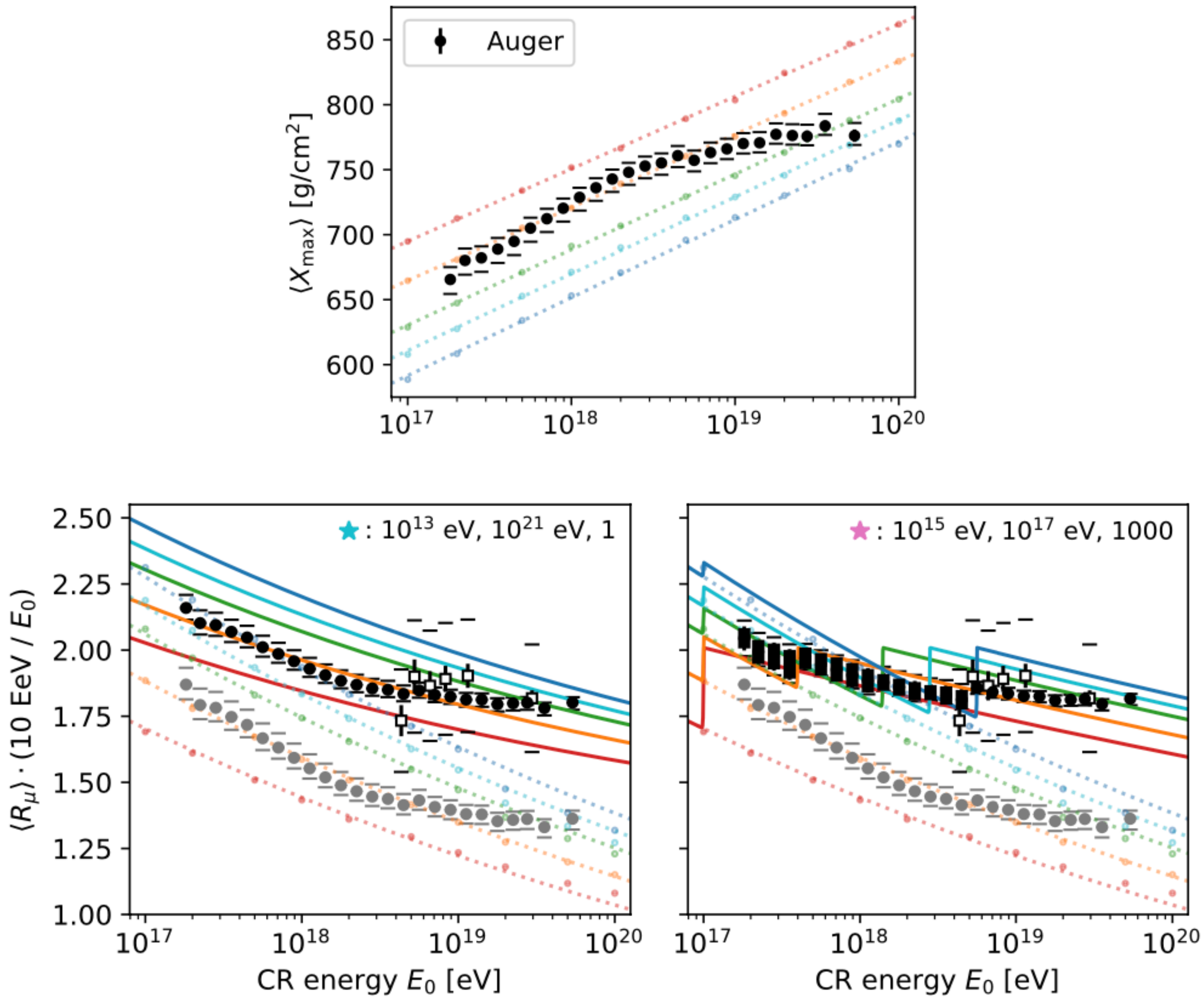

Figure 6. Composition inference from Auger data (error bars) on $\langle X_{\max}\rangle$ (top) and $\langle R_\mu\rangle$ (bottom) using EPOS-LHC and the strangeball model. The strangeball model (solid lines) leaves $\langle X_{\max}\rangle$ unaffected, data on which (black error bars) can thus be interpreted within the Standard Model (dotted lines). In the bottom plots a direct comparison with $\langle R_\mu\rangle$ data (white square error bars) follows from mapping $\langle X_{\max}\rangle$ data to $\langle R_\mu\rangle$ within the Standard Model (gray error bars) and the following two strangeball scenarios (black error bars): $E_{\min} = 10^{13}$ eV, $E_{\max} = 10^{21}$ eV and $n = 1$ (bottom left), and $E_{\min} = 10^{15}$ eV, $E_{\max} = 10^{17}$ eV and $n = 1000$ (bottom right). The line colors correspond to various nuclei: proton (red), helium (orange), nitrogen (green), silicon (cyan), and iron (blue).

$X_{\max}$ mapping to R_μ in Standard Model (gray) and two strange ball models (black) versus various pure compositions (lines)

Strangeball parameter compatibility

A χ^2 statistical analysis with the Pierre Auger data in parameter space $E_{\min}$, $E_{\max}$, and n.

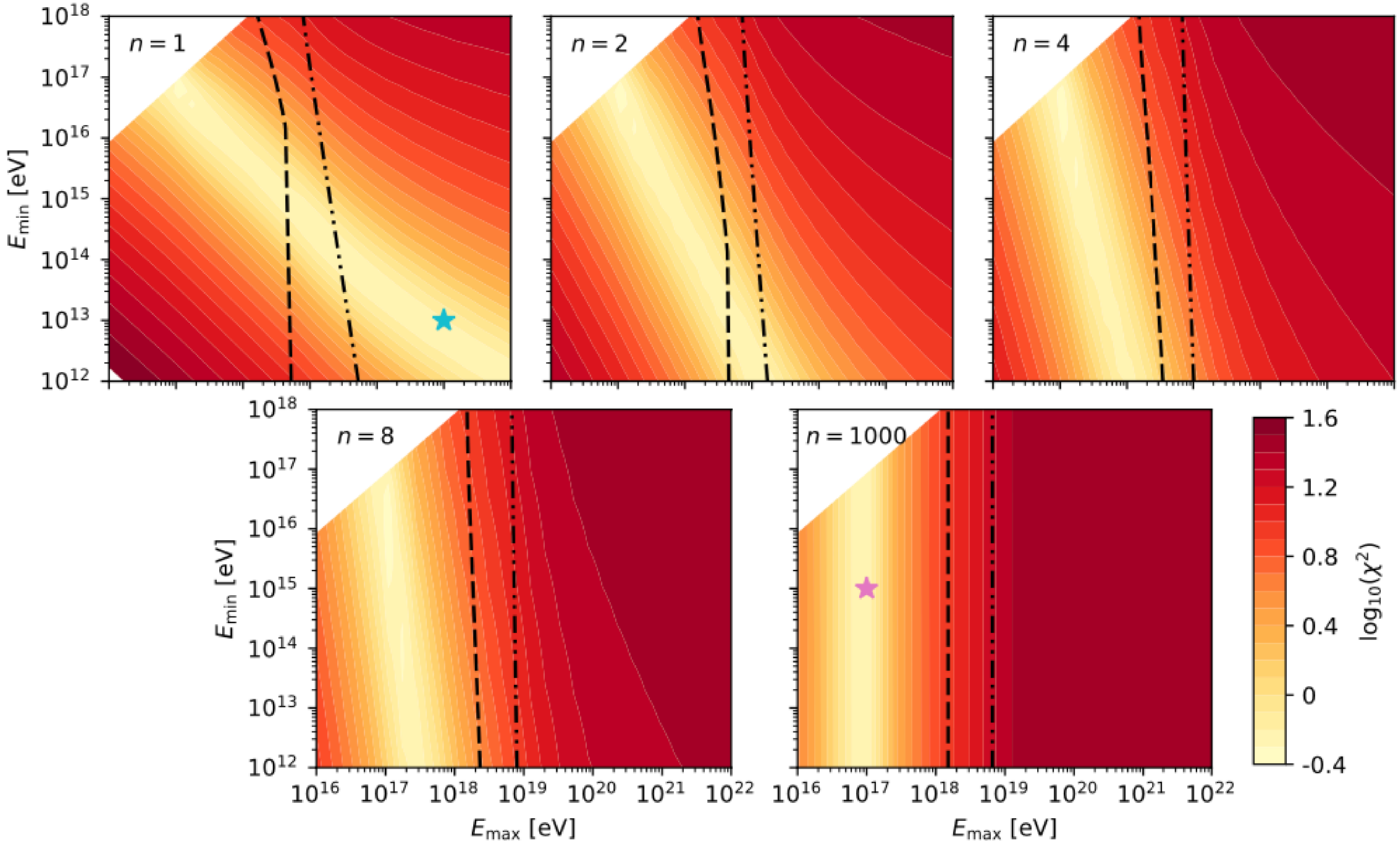

Figure 7. Strangeball parameter-space exploration of the compatibility of the composition inference of Auger data on $\langle X_{\max} \rangle$ and $\langle R_\mu \rangle$ as quantified by the test statistic χ^2 (eq. (5.1)) for EPOS-LHC. A lower χ^2 implies a better compatibility. The inset stars correspond to the central (cyan) and right (purple) plots in figure 6. The black lines are lower limits on $E_{\max}$ derived from data on the muon fluctuations.

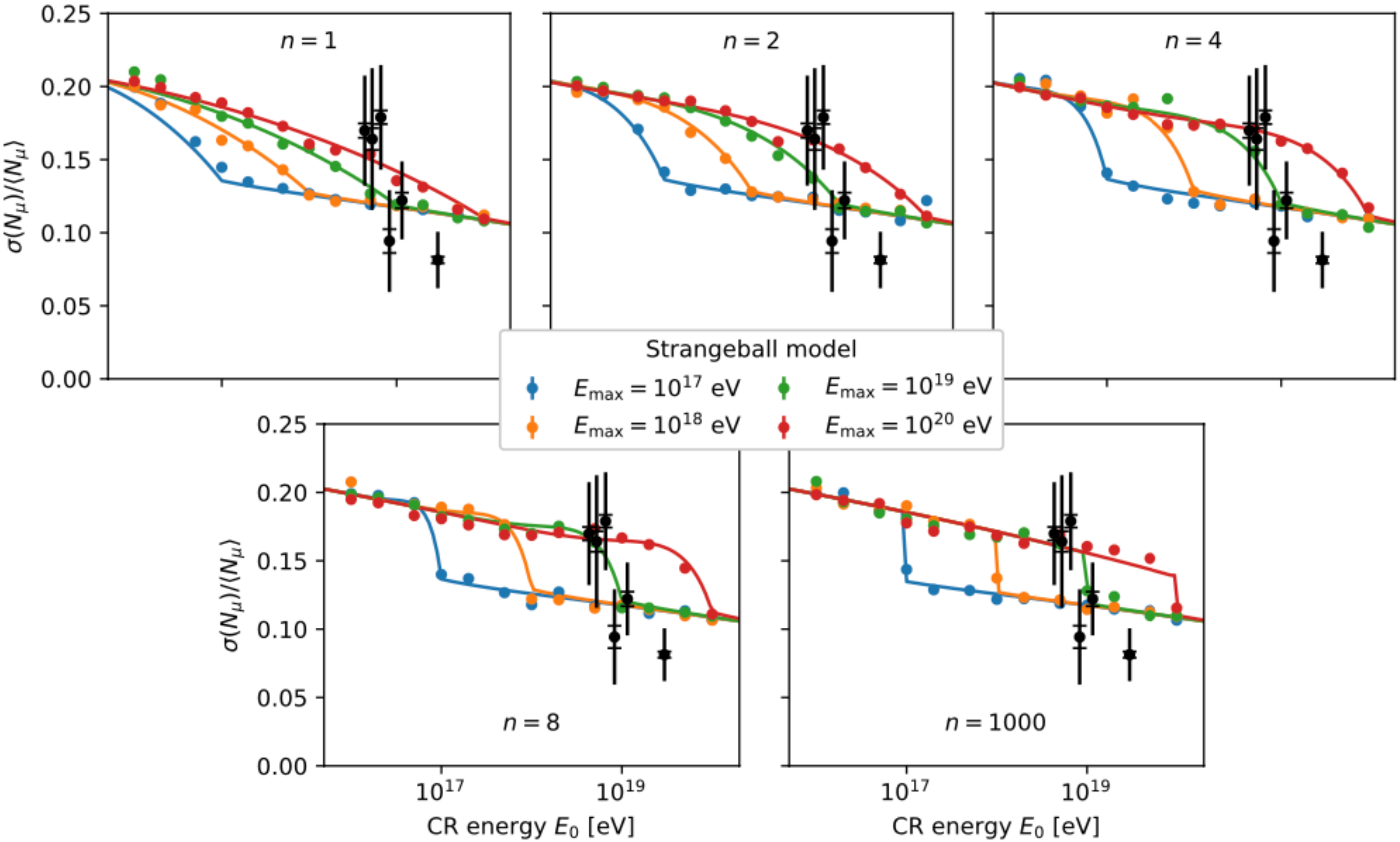

Figure 13. Energy dependence of the relative muon fluctuations from strangeball-extended CONEX simulations with EPOS-LHC (colored points) for various strangeball settings: $E_{\rm min} = 10^{15}$ eV is fixed, while $E_{\rm max}$ (colors) and n (panels) vary. These simulations are fitted with our model (colored lines, eq. (A.7)), whose fit parameters are summarized in table 3. The black data points are from the Pierre Auger Observatory as presented at the ICRC in 2019 [51].

Strangeball parameters

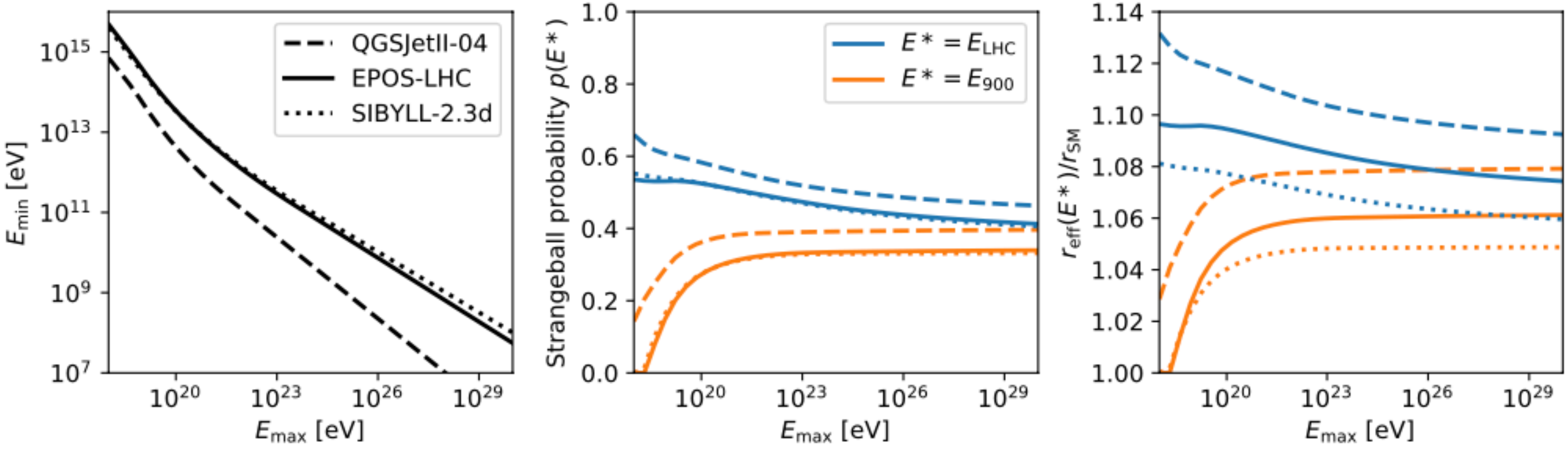

Figure 8. *Left:* strangeball settings resolving the muon puzzle without violating constraints from the muon fluctuations (i.e. $E_{\rm max} \gtrsim 10^{19}\,{\rm eV}$). *Center and right:* conversion of these strangeball settings to the strangeball-initiation probability (center, eq. (2.2)) and effective enhancement of the hadronic energy fraction (right, eq. (4.2)) at LHC (blue, $E_{\rm LHC} \approx 10^{17}\,{\rm eV}$) and Tevatron (orange, $E_{\rm Tev} \approx 10^{15}\,{\rm eV}$) energies.

Implications for LHC Measurements

The hadronic energy fraction r is not directly measurable -> other observables need to be considered.

Some notation:
energies and momenta refer to a hadron
transverse mass $m_T = \left(m^2 + p_\perp^2\right)^{1/2}$

rapidity $y = \frac{1}{2}\ln\left(\frac{E+p_z}{E-p_z}\right)$

in the center of mass frame: Feynman x: $x_F = \frac{p_z}{p_{z,\max}}$ with $p_{z,\max} \simeq E_{\mathrm{CM}} \simeq s^{1/2}/2$

$E = m_\perp \cosh y\,, p_z = m_\perp \sinh y\,, x_F = \tanh y$

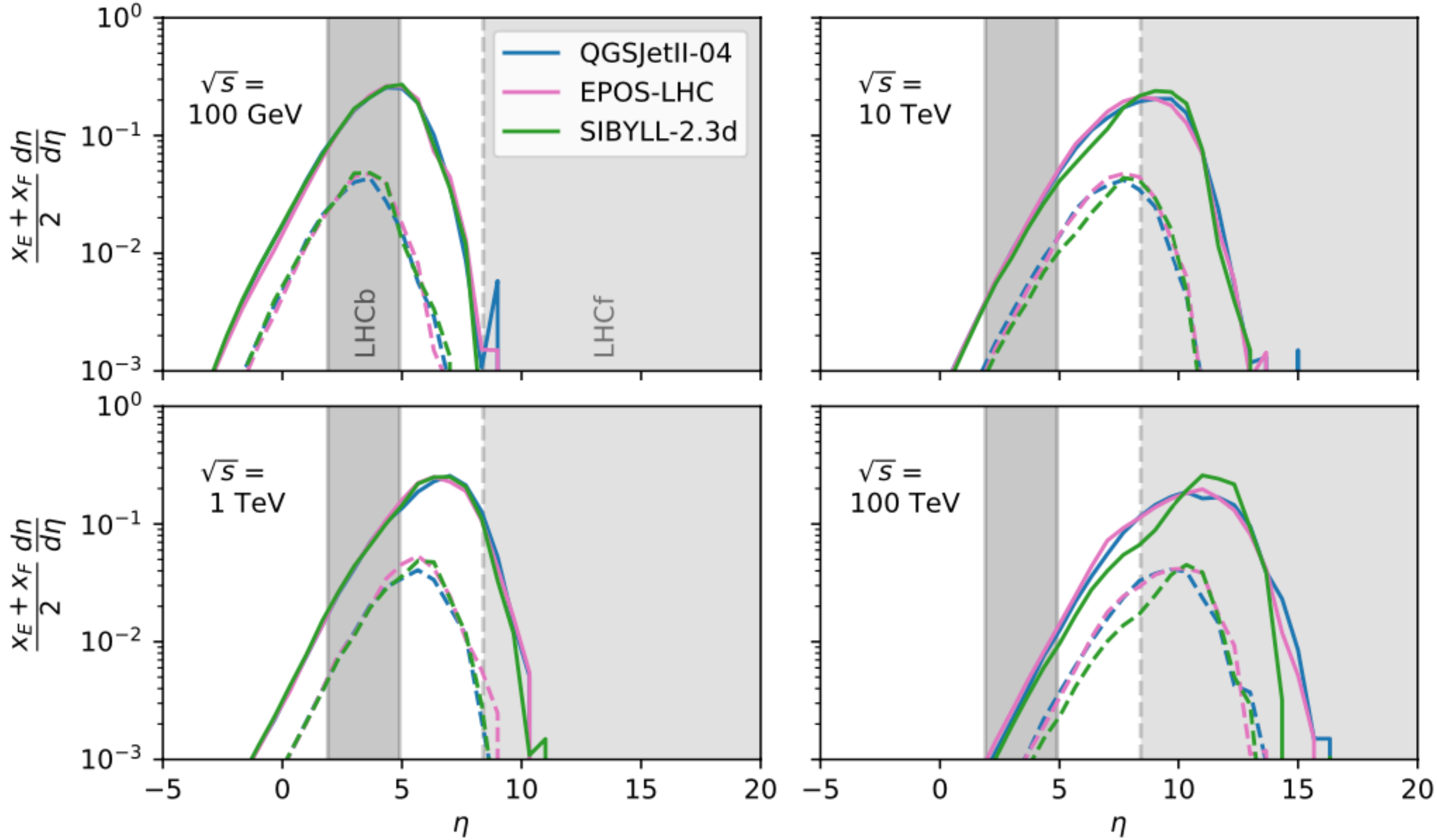

Figure 9. Weighted pseudorapidity distributions of all (solid lines) and EM-only (including π^0, dashed lines) secondaries from proton-proton collisions at various center-of-mass energies for the three hadronic interaction models, computed with CRMC. The weight corresponds to the fraction of projectile energy carried by secondaries when boosted to the fixed-target rest frame, given by eq. (6.1). The pseudorapidity acceptance regions of LHCb ($1.9 < \eta < 4.9$ [7]) and LHCf ($|\eta| > 8.4$ [70]) are indicated in gray.

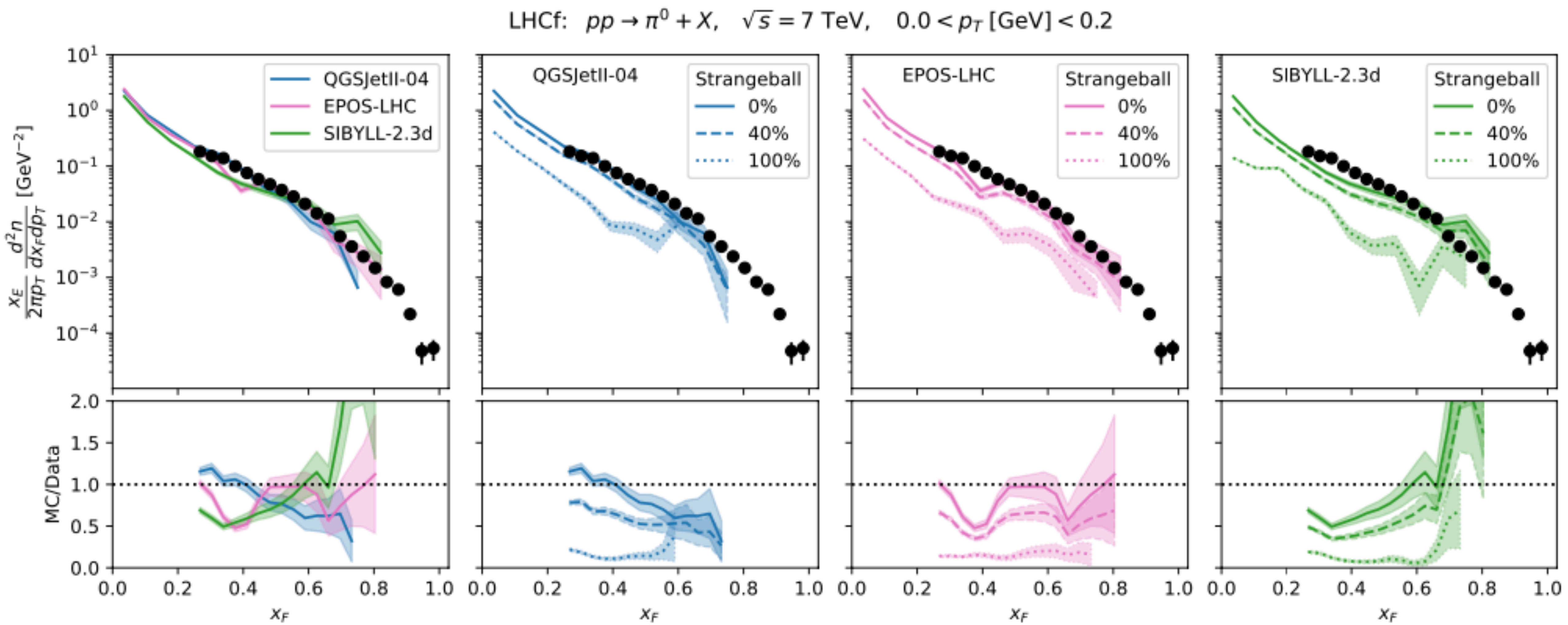

Figure 10. The neutral pion yield from proton-proton collisions at $\sqrt{s} = 7\,\text{TeV}$ as measured by the LHCf detector [70] (data points) and retrieved from various models with CRMC (lines), for the p_T-range of 0.0 to 0.2 GeV. For clarity, we separately visualize the effect of 40% and 100% strangeballs for each of the hadronic interaction models. The bands correspond to $1\,\sigma$ Monte Carlo uncertainties.

40% strange balls are within model uncertainties

Note that η and $x_F = 2p_z/s^{1/2}$ are independent variables so that at very forward directions (large η) measurements at small x_F are also possible

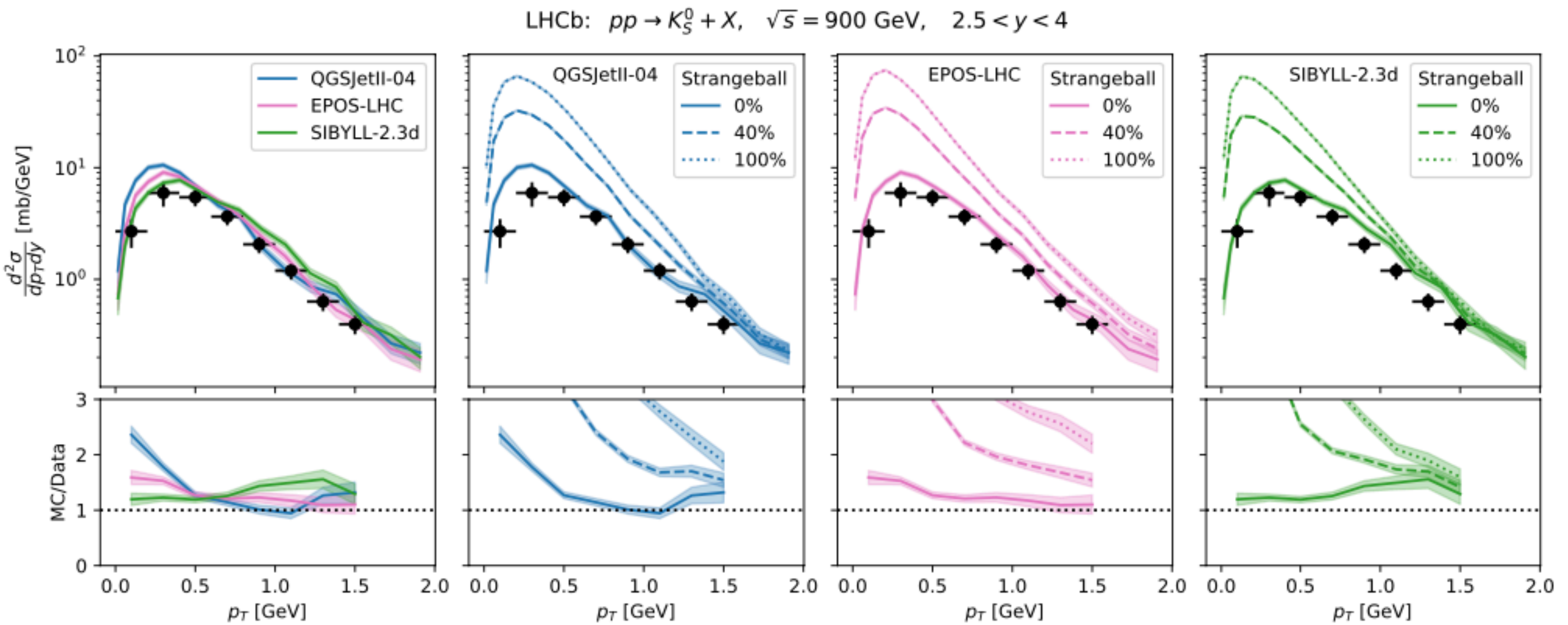

Figure 11. The K_S^0 p_T-spectrum from proton-proton collisions at $\sqrt{s} = 900\,\text{GeV}$ as measured by the LHCb detector [71] (data points) and retrieved from various models with CRMC (lines), for the rapidity range of 2.5 to 4. For clarity, we separately visualize the effect of 40% and 100% strangeballs for each of the hadronic interaction models. The bands correspond to $1\,\sigma$ Monte Carlo uncertainties.

This requires $E_{\rm min} \gtrsim 4 \times 10^{14}$ eV; maybe changed if pion interactions are taken into account

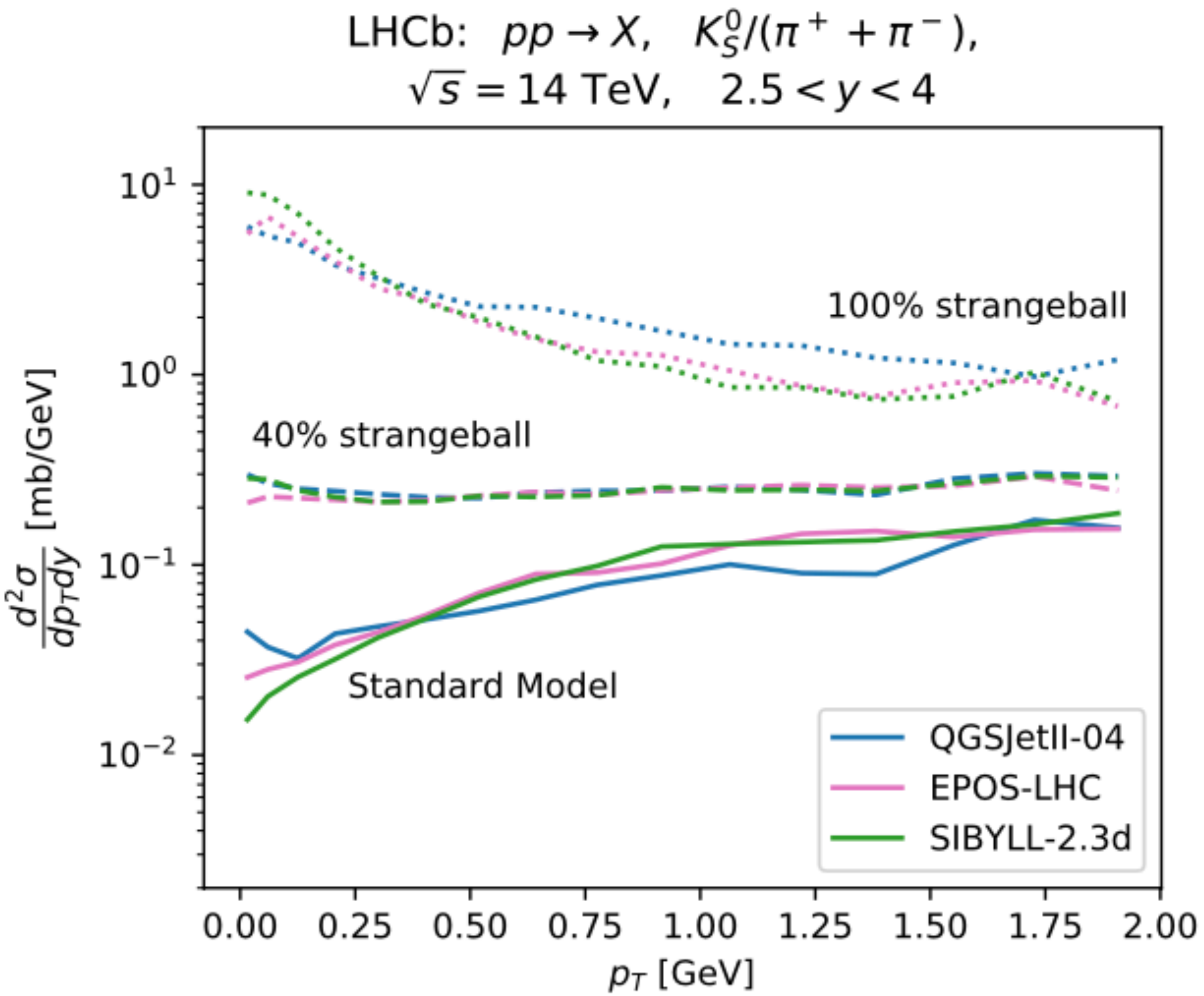

Figure 12. Ratio of K_S^0 to charged pion p_T-spectra from proton-proton collisions at $\sqrt{s} = 14\,\text{TeV}$, computed with CRMC, that could be measured by the LHCb detector to test the strangeball solution to the muon puzzle.

strong discriminator for strange ball model hopefully measurable in the near future by LHCb

Core-corona model

Baur et al., Phys. Rev. D 107 (2023) 094031

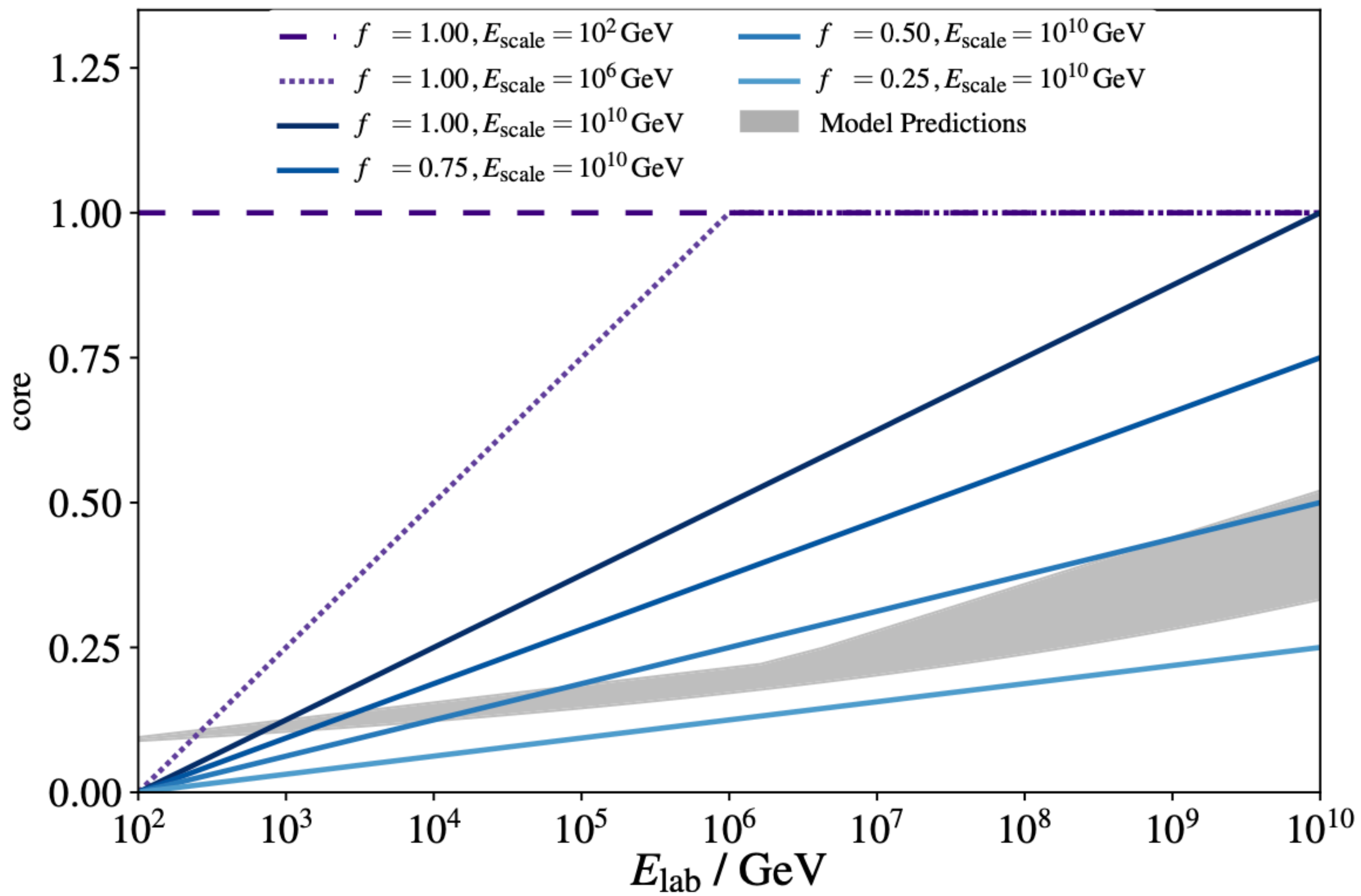

FIG. 5. Different energy evolutions probed for ω_{core}. The solid lines represent changing the scale f_ω of the effect, while the dashed lines also indicate the effect of changing E_{scale}. The shaded area is based on Fig. 4 motivate by ALICE data and current predictions on particle densities of the EPOS3 model.

The core weight energy dependence extracted from ALICE data on strangeness are strongly extrapolated in energy.

Possible test proposed through neutrino flux measurements @FASERν and the Forward Physics Facility (FPF)

Outlook: Model Uncertainties on Air Shower Muon Content

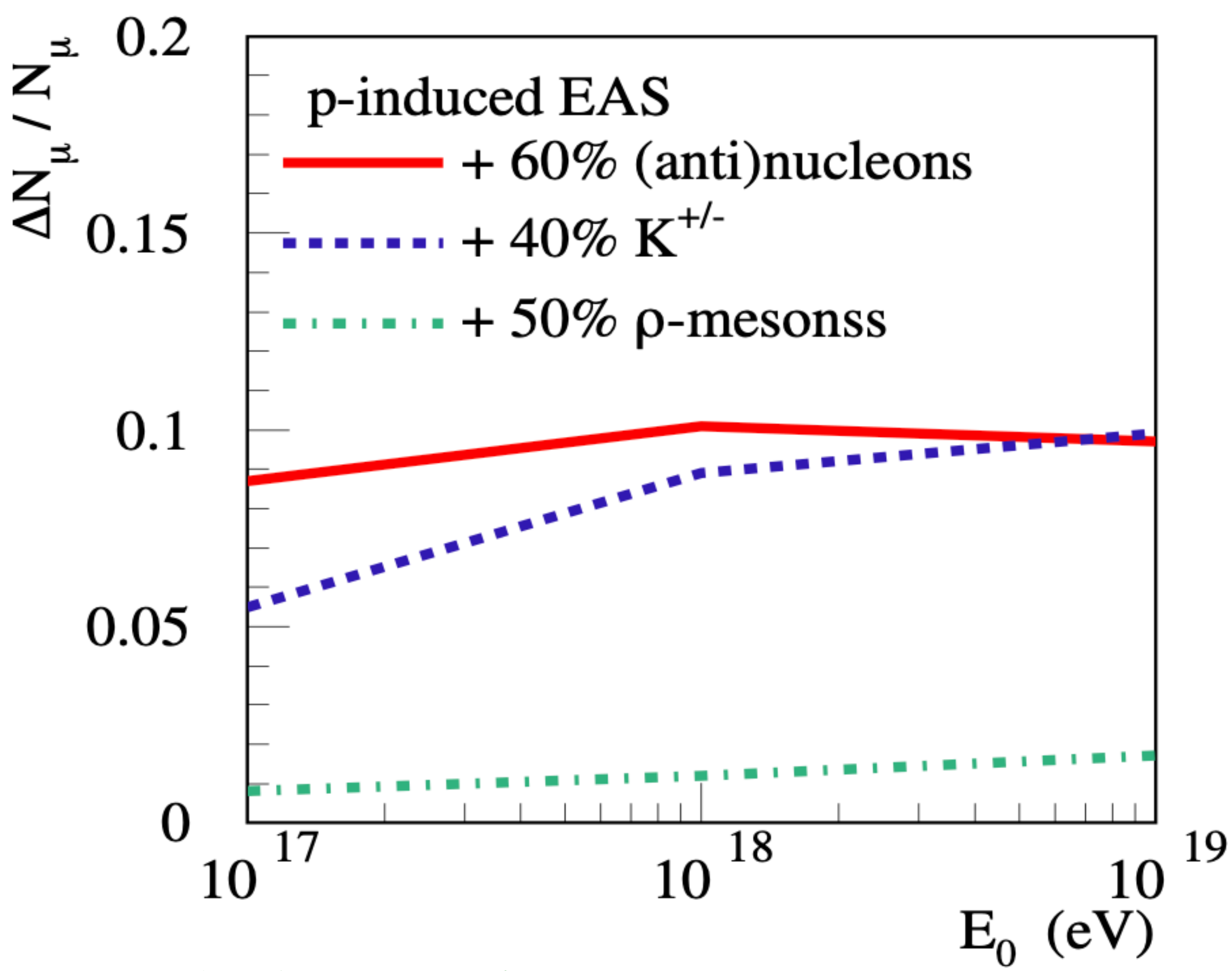

preliminary work by Ostapchenko and Sigl

Figure **7**: Energy dependence of the N_μ enhancement ($E_\mu > 1$ GeV, sea level), relative to the default QGSJET-III results, for proton-induced EAS for the considered modifications of particle production in the QGSJET-III model: enhancement of (anti)nucleon (solid line), kaon (dashed line), and ρ-meson (dotted-dashed line) production.

calibrated on NA61 data

Conclusions

1.) The formation of a plasma in the context of the fireball model ($f_{\text{thresh}} < 1$) is inconsistent with the Pierre Auger data because of tensions between average X_{max} and its fluctuations (due to enhanced inelasticity and multiplicity)

2.) Strangeball model can work if no plasma forms but strangeness is enhanced: For example, a sudden turn-on around 10^{17} eV or a gradual turn-on below 10^{14} eV (40% strangeballs with 5-9% hadronic increase) is not yet in contradiction with LHC data. Latter case is favoured by muon fluctuation data and can be probed at colliders

3.) The strangeball and core-corona models are similar, but in the core corona model both core and corona contribute at the same time, whereas a strange ball is formed only with some probability -> could influence the fluctuations of air shower variables

4.) A possible probe of the strangeball model at LHCb is the K_S^0 to charged pion p_T spectrum